JCTC Journal of Chemical Theory and Computation

Article

pubs.acs.org/JCTC

The Symmetrical Quasi-Classical Model for Electronically Non-Adiabatic Processes Applied to Energy Transfer Dynamics in Site-Exciton Models of Light-Harvesting Complexes

Stephen J. Cotton*,†,‡ and William H. Miller*,†,‡

†Department of Chemistry and Kenneth S. Pitzer Center for Theoretical Chemistry, University of California, Berkeley, California 94720, United States

‡Chemical Sciences Division, Lawrence Berkeley National Laboratory, Berkeley, California 94720, United States

ABSTRACT: In a recent series of papers, it has been illustrated that a symmetrical quasi-classical (SQC) windowing model applied to the Meyer−Miller (MM) classical vibronic Hamiltonian provides an excellent description of a variety of electronically non-adiabatic benchmark model systems for which exact quantum results are available for comparison. In this paper, the SQC/MM approach is used to treat energy transfer dynamics in site-exciton models of light-harvesting complexes, and in particular, the well-known 7-state Fenna−Mathews−Olson (FMO) complex. Again, numerically "exact" results are available for comparison, here via the hierarchical equation of motion (HEOM) approach of Ishizaki and Fleming, and it is seen that the simple SQC/MM approach provides very reasonable agreement with the previous HEOM results. It is noted, however, that unlike most (if not all) simple approaches for treating these systems, because the SQC/MM approach presents a fully atomistic simulation based on classical trajectory simulation, it places no restrictions on the characteristics of the thermal baths coupled to each two-level site, e.g., bath spectral densities (SD) of any analytic functional form may be employed as well as discrete SD determined experimentally or from MD simulation (nor is there any restriction that the baths be harmonic), opening up the possibility of simulating more realistic variations on the basic site-exciton framework for describing the non-adiabatic dynamics of photosynthetic pigment complexes.

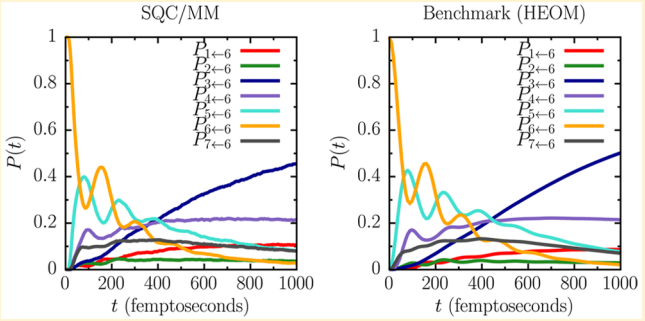

1. INTRODUCTION

The Meyer−Miller (MM) classical vibronic Hamiltonian[1] maps the coupled dynamics of nuclear and electronic degrees of freedom (DOF) in non-adiabatic processes onto a set of classical "electronic" oscillators with each oscillator representing the occupation of the various electronic states. In a recent series of papers, a symmetrical quasi-classical (SQC) windowing model[2] has been described and applied to the MM Hamiltonian to "quantize" these electronic DOF both initially and finally.[3] It was found that this approach provides a very reasonable description of non-adiabatic dynamics exhibited in a suite of standard benchmark model problems for which exact quantum mechanical (QM) results are available for comparison. Among the examples were systems exhibiting strong quantum coherence effects and systems representative of condensed-phase non-adiabatic dynamics, including some that other simple approaches have difficulty in describing correctly (e.g., the asymmetric spin-boson problem[3] and the inverted regime[4] in electron transfer processes[5]).

It was also explained in these recent papers how various aspects of the SQC/MM model are appealing from a theoretical perspective, e.g., it has a straightforward theoretical justification (see section 2 below), and by providing an equivalent treatment of the electronic and the nuclear DOF (i.e., via classical mechanics), it is able to describe "quantum" coherence and decoherence without resorting to any "add ons" to the theory. The (classical) time evolution of the nuclear and electronic DOF is continuous at all times (as it is QM'ly), and it gives equivalent results whether implemented in adiabatic or diabatic representations. Furthermore, the SQC method of quantizing the electronic DOF leads to detailed balance being described correctly, or at least approximately so.[6] It was also emphasized that though the equations of motion that result from the MM Hamiltonian are "Ehrenfest", in that the force on the nuclei at any time is the coherent average of that over all electronic states, the fact that zero point energy is included in the electronic oscillators means that there is an ensemble of trajectories for each initial state (rather than only one trajectory as in the "Ehrenfest method" itself) and that each final electronic state is determined by its own fraction of that ensemble.[7] The approach thus does not suffer from the well-known "Ehrenfest defect" of having all final electronic states determined by one (average) nuclear trajectory.

However, despite providing a reasonably accurate and theoretically sound treatment of electronically non-adiabatic

Received: December 14, 2015
Published: January 13, 2016

DOI: 10.1021/acs.jctc.5b01178
J. Chem. Theory Comput. 2016, 12, 983−991

phenomena, because the SQC/MM approach is trajectory-based and employs only "ordinary" classical mechanics, it is quite straightforward to incorporate into the framework of a standard classical MD simulation. One effectively has only several additional vibrational-like DOF, one for each electronic state, which are propagated along with the nuclear DOF via Hamilton's equations that result from the MM Hamiltonian.

The SQC/MM model is of course an approximation and will thus undoubtedly perform better in some applications than in others; as such, we have sought to test it on as many diverse benchmark problems as possible and continue to seek ways to improve it as necessary. Most recently, for example, it was also pointed out that although the Meyer−Miller (MM) Hamiltonian is an exact nuclear-electronic Hamiltonian operator if all DOF are treated QM'ly (see section 2.1 below), there are in fact other formally exact representations, and although these alternative representations are QM'ly equivalent to the MM Hamiltonian, they are *not* equivalent to it in their classical limits, i.e., when quantum operators (in these exact Hamiltonians) are replaced with ordinary classical variables. It was in this spirit that we sought to explore one of these alternative classical representations—in particular, a classical spin-mapping (SM) model[7]—which was then "quantized" in the same SQC fashion as the MM Hamiltonian. This work showed that the new SQC/SM model works reasonably well, but that it does not perform quite as well as the previous SQC/MM model over the suite of benchmark problems that were used to compare the two approaches. Because the SQC/SM model is new and equally justifiable QM'ly, it remains to be seen whether this is generally true for all problems.

In this paper, the SQC/MM approach for treating electronically non-adiabatic processes is applied, in its now standard formulation (without any modifications), to site-exciton models of light-harvesting complexes, starting with the 2-site/2-state examples used by Ishizaki and Fleming to develop their hierarchical equation of motion (HEOM) approach[8] and then moving on to the well-known 7-state site-exciton model of the Fenna−Mathews−Olson (FMO) complex (also treated by Ishizaki and Fleming[9] with the HEOM method). Because the HEOM approach is numerically exact (if enough terms are maintained in the hierarchical expansion), this provides another avenue for benchmarking the SQC/MM model. It is noted, however, that once validated, the SQC/MM technique, because it constitutes a fully atomistic classical trajectory simulation, is not limited to particular forms of bath spectral density (SD) functions and does not even require that the bath environments coupled at each site be harmonic. It is this generality that is exciting because many real biochemical systems of interest are not well-described by SDs having simple analytic functional forms, and (of course), even the assumption that each site's environment is harmonic is not always a good one.

This paper is organized as follows: section 2 provides a brief overview of the classical Meyer−Miller (MM) vibronic Hamiltonian and its quantization within the symmetrical quasi-classical (SQC) framework (a short list of steps for the SQC procedure is given in Appendix A). Results of applying the SQC/MM approach are presented in section 3, beginning with a description of the site-exciton models to be considered; results for the case of 2-sites/pigments are given in section 3.2 compared against Ishizaki and Fleming's benchmark HEOM calculations for 8 different parameter regimes, and section 3.3 follows with a treatment of the 7-site FMO problem (again with HEOM results shown for comparison). Our conclusions are summarized in section 4.

2. THEORY

The SQC/MM methodology consists of two basic ingredients: (i) the Meyer−Miller (MM) classical vibronic Hamiltonian, which treats nuclear and electronic DOF in a consistent (albeit classical) unified framework, and (ii) a symmetrical quasi-classical (SQC) windowing procedure that is used to "quantize" the electronic DOF embodied as classical oscillators in the MM Hamiltonian (which is an approximate version of Bohr−Sommerfeld quantization of classical action variables). Inputs to the SQC/MM model are the electronic potential energy surfaces (PES) for the non-adiabatic system to be simulated, which may come, e.g., from rigorous "quantum chemistry", less-rigorous density functional theory (DFT), or from a semi-empirical force field as generally used in biomolecular simulation. Notably, these PES "inputs" may represent adiabatic or diabatic electronic states, as there are both adiabatic and diabatic versions of the MM Hamiltonian that are formally equivalent[3] (the latter being applied in this paper). The following two subsections briefly discuss these two ingredients.

2.1. Summary of the Meyer−Miller Hamiltonian. The physical picture of the electronic DOF provided by the classical MM Hamiltonian is that each electronic state's occupation is represented by a classical harmonic oscillator, the first excited state and the ground state of each oscillator representing, respectively, whether the corresponding electronic state is occupied or unoccupied. In Cartesian oscillator variables, the MM classical vibronic Hamiltonian is

$$H(\mathbf{P}, \mathbf{R}, \mathbf{p}, \mathbf{x}) = \frac{|\mathbf{P}|^2}{2\mu} + \sum_k \left(\frac{1}{2}p_k^2 + \frac{1}{2}x_k^2 - \gamma\right)H_{k,k}(\mathbf{R}) + \sum_{k<k'} (p_k p_{k'} + x_k x_{k'})H_{k,k'}(\mathbf{R}) \tag{1}$$

where $\frac{|\mathbf{P}|^2}{2\mu}$ is the nuclear kinetic energy, $\{x_k, p_k\}$ are the coordinates and momenta of the "electronic" oscillators, $\{H_{kk}(\mathbf{R})\}$ are the diabatic (in this case) electronic PES (parametrically dependent on the nuclear coordinates $\mathbf{R}$), $H_{k,k'\neq k}(\mathbf{R})$ are the non-adiabatic couplings (also potentially depending on $\mathbf{R}$), and γ is a fixed zero-point energy (ZPE) parameter chosen between 0 and $\frac{1}{2}$. An equivalent expression in terms of classical harmonic oscillator action-angle variables is

$$H(\mathbf{P}, \mathbf{R}, \mathbf{n}, \mathbf{q}) = \frac{|\mathbf{P}|^2}{2\mu} + \sum_k n_k H_{k,k}(\mathbf{R}) + 2\sum_{k<k'} \sqrt{n_k + \gamma}\sqrt{n_{k'} + \gamma}\cos(q_k - q_{k'})H_{k,k'}(\mathbf{R}) \tag{2}$$

and the Cartesian and action-angle electronic variables are related by the canonical transformation

$$p_k = -\sqrt{2(n_k + \gamma)}\sin(q_k) \tag{3a}$$

$$x_k = \sqrt{2(n_k + \gamma)}\cos(q_k) \tag{3b}$$

or inversely

$$n_k = \frac{1}{2}p_k^2 + \frac{1}{2}x_k^2 - \gamma \tag{4a}$$

DOI: 10.1021/acs.jctc.5b01178
J. Chem. Theory Comput. 2016, 12, 983−991

$$q_k = -\tan^{-1}\left(\frac{p_k}{x_k}\right) \tag{4b}$$

The classical action variables $\{n_i\}$ in conjunction with the ZPE γ-parameter determine the amount of harmonic excitation and are, of course, the classical analogues of the vibrational quantum numbers; initially and finally, they are what are "quantized" about their QM integer values (of 0 or 1) within the SQC framework (Bohr−Sommerfeld quantization). The electronic configuration may thus be viewed as a single harmonic excitation that moves among the different oscillators (each representing an electronic state) according to Hamiltonian's equations as applied to the Hamiltonian given by either eqs 1 or 2. Consistent with this picture, the classical dynamics preserves the sum of the actions/occupations, $\sum_k \dot{n}_k = 0$, which is conservation of total probability.

There are (at least) two distinct ways to arrive at the Meyer−Miller classical Hamiltonian given in eq 1: the more rigorous approach[10] is to begin with the exact QM Hamiltonian operator in second-quantized form,

$$\hat{H} = \frac{|\hat{P}|^2}{2\mu} + \sum_{k,k'} \hat{a}_k^\dagger H_{k,k'}(\hat{R})\hat{a}_{k'} \tag{5}$$

and to represent the creation/annihilation operators in terms of the raising/lowering operators of harmonic oscillators (i.e., bosons, hence "Schwinger bosonization")

$$\hat{a}_k^\dagger = \frac{1}{\sqrt{2}}(\hat{x}_k - i\hat{p}_k),\ \ \hat{a}_k = \frac{1}{\sqrt{2}}(\hat{x}_k + i\hat{p}_k) \tag{6}$$

which gives

$$\begin{aligned}\hat{H} &= \frac{|\hat{P}|^2}{2\mu} + \sum_{k,k'} \frac{1}{2}(\hat{p}_k\hat{p}_{k'} + \hat{x}_k\hat{x}_{k'} + i[\hat{x}_k, \hat{p}_{k'}])H_{k,k'}(\hat{R}) \\ &= \frac{|\hat{P}|^2}{2\mu} + \sum_k \left(\frac{1}{2}\hat{p}_k^2 + \frac{1}{2}\hat{x}_k^2 - \frac{1}{2}\right)H_{k,k'}(\hat{R}) \\ &\quad + \sum_{k<k'} (\hat{p}_k\hat{p}_{k'} + \hat{x}_k\hat{x}_{k'})H_{k,k'}(\hat{R})\end{aligned} \tag{7}$$

(in the last step, taking advantage of the commutation relation $[\hat{x}_k, \hat{p}_{k'}] = i\delta_{k,k'}$). Eq 1 is then simply the classical limit one obtains by replacing the QM operators with ordinary classical variables (i.e., $\hat{\mathbf{P}},\hat{\mathbf{R}},\hat{\mathbf{p}},\hat{\mathbf{x}} \rightarrow \mathbf{R},\mathbf{P},\mathbf{p},\mathbf{x}$) and introducing the variable γ-parameter.

The original, more intuitive/heuristic approach[1] is to define the classical electronic Hamiltonian as the expectation value of the electronic energy expanded in a basis of the electronic states in question ($|\psi_{el}\rangle = \sum_k c_k|k\rangle$) and to express the expansion coefficients $\{c_k\}$, the (time-dependent) complex electronic amplitudes, in terms of real amplitudes and phases (i.e., time-dependent actions and angles) with the relationship $c_k \equiv \sqrt{n_k}e^{-iq_k}$. This gives

$$\begin{aligned}H_{el}(\mathbf{R}, \mathbf{n}, \mathbf{q}) &\equiv \sum_{k,k'} c_k^* H_{k,k'}(\mathbf{R})c_{k'},\ (\equiv \langle\psi_{el}|\hat{H}_{el}|\psi_{el}\rangle) \\ &= \sum_{k,k'} \sqrt{n_k n_{k'}}\cos(q_k - q_{k'})H_{k,k'}(\mathbf{R}) \\ &= \sum_k n_k H_{k,k}(\mathbf{R}) + 2\sum_{k<k'} \sqrt{n_k n_{k'}}\cos(q_k - q_{k'})H_{k,k'}(\mathbf{R})\end{aligned} \tag{8}$$

A "Langer (like) modification" to the coupling terms, $n_k \rightarrow n_k + \frac{1}{2}$ and adding the classical nuclear kinetic energy then gives eq 2 (whereby the canonical transformation in eqs 3 and 4 gives eq 1, so long as γ is taken to be $\frac{1}{2}$ (in eqs 1 and 2), as it was in the original version.[1]

The justification for this heuristic development (and the insight gained from it) is that, with the definition of classical actions and angles $\{n_k, q_k\}$ as the amplitudes and phases of the complex QM electronic amplitudes $\{c_k\}$, for a given nuclear trajectory, $\mathbf{R}(t)$, the classical trajectories generated in terms of $\{n_k, q_k\}$ (using Hamilton's equations with eq 8) are exactly equivalent to the propagation of the $\{c_k\}$ with the electronic Schrödinger equation (note $\hbar = 1$ throughout):

$$i\frac{\mathrm{d}}{\mathrm{d}t}c_k(t) = \sum_{k'} H_{k,k'}(\mathbf{R}(t))\cdot c_{k'}(t) \tag{9}$$

(This may be verified by substituting $c_k = \sqrt{n_k}e^{-iq_k}$ into eq 9 and comparing to Hamilton's equations for the actions and angles $\dot{n}_k = -\frac{\partial H_{el}}{\partial q_k}$, $\dot{q}_k = \frac{\partial H_{el}}{\partial n_k}$). In other words, the *classical* Meyer−Miller Hamiltonian may be viewed as a rewriting of the electronic Schrödinger equation in terms of classical action-angle variables (or Cartesian components), which is why what is conventionally viewed as "quantum coherence" is captured in the purely classical motion of these electronic oscillators. See, for example, the problems treated in ref 3 (as well as the results in this paper).

For the nuclear DOF, application of Hamilton's equations, $\dot{P} = -\frac{\partial H}{\partial \mathbf{R}}$, $\dot{R} = \frac{\partial H}{\partial \mathbf{P}}$, to eq 1 (or eq 2) gives the force on the nuclei, $\mu\ddot{R}(t) = -\frac{\partial H}{\partial \mathbf{R}}$, in view of eq 8 as

$$\mu\ddot{R}(t) = -\sum_{k,k'} c_k^* \frac{\partial H_{k,k'}(\mathbf{R})}{\partial \mathbf{R}} c_{k'}\left(\equiv -\frac{\partial}{\partial \mathbf{R}}\langle\psi_{el}|\hat{H}_{el}|\psi_{el}\rangle\right) \tag{10}$$

i.e., as the electronic occupation-weighted average of the forces given from the different electronic PES (which are the inputs to the model). This is in fact the "Ehrenfest *force*," but for (relatively subtle) reasons explained in detail in ref 7, the SQC/MM approach (being based on the MM Hamiltonian) overcomes the well-known and inherent deficiencies of the Ehrenfest *approach*. The 7-state FMO problem treated in this paper provides an illustrative example.

2.2. Summary of Symmetrical Quasi-Classical Quantization. The symmetrical quasi-classical (SQC) quantization model is that the classical actions (which are the classical analogues of the quantum numbers) corresponding to the DOF of interest are "quantized" symmetrically (i.e., initially and finally) by defining "window functions"—essentially prelimit delta functions about the relevant integer values of the action variables—and applying one at the beginning of a classical trajectory simulation as well as at the end. This is an approximate implementation of "Bohr−Sommerfeld quantization" as incorporated in Miller's "classical S-matrix" theory.[11] The window functions are narrower than in the original quasi-classical approach,[12] and by applying them symmetrically, microscopic reversibility is enforced (something not true of the original quasi-classical trajectory procedure).

The SQC concept was initially demonstrated for the initial and final vibrational states in reactive scattering calculations for $H + H_2$, and it was seen to provide an easy improvement over

DOI: 10.1021/acs.jctc.5b01178
J. Chem. Theory Comput. 2016, 12, 983−991

results obtained by the traditional quasi-classical trajectory (QCT) procedure.[2] In modeling the much more interesting case of electronically non-adiabatic processes, the SQC quantization procedure is applied to the electronic oscillator DOF of the MM Hamiltonian whose excitations (as described above) represent the occupations of the electronic states. This is done by applying to each classical action n in the MM model a histogram window function

$$w_N(n) = \frac{1}{2\gamma} h(\gamma - |n - N|), \text{ where } h(x) \equiv \begin{cases} 0 & x < 0 \\ 1 & x \geq 0 \end{cases} \tag{11}$$

which has width 2γ and is centered at the quantum values of the classical actions $N \in \{1,0\}$ (occupied, unoccupied). Eq 11 windows a single electronic DOF (constraining the associated action n to lie within $[N - \gamma, N + \gamma]$). For $F = 2$ electronic states, the quantum values of the actions corresponding to state $|1\rangle$ being occupied are $(N_1,N_2) = (1, 0)$, and likewise, $(N_1,N_2) = (0, 1)$ correspond to state $|2\rangle$ being occupied. Thus, the full window functions representing states $|1\rangle$ and $|2\rangle$ are

$$W_{|1\rangle}(n_1, n_2) = w_1(n_1)\cdot w_0(n_2) \tag{12a}$$

$$W_{|2\rangle}(n_1, n_2) = w_0(n_1)\cdot w_1(n_2) \tag{12b}$$

Generalizing, for an arbitrary F number of electronic states/DOF, the action window function representing state $|k\rangle$ is

$$W_{|k\rangle}(\mathbf{n} \equiv n_1, \ldots n_k, \ldots n_F) = w_1(n_k)\cdot \prod_{k' \neq k}^{F} w_0(n_{k'}) \tag{13}$$

where each $w_{N_k}(n_k)$ is the single DOF histogram window function in eq 11.

Within this SQC windowing framework, calculating the probability of an electronically non-adiabatic transition between initial state $|i\rangle$ and final state $|f\rangle$ amounts to Monte Carlo evaluation of the following phase space average for all energetically feasible final states $|k\rangle$

$$\tilde{P}_{|k\rangle \leftarrow |i\rangle}(t) = \frac{1}{(2\pi)^{G+F}} \int d\mathbf{P}_0\, d\mathbf{R}_0\, d\mathbf{n}_0\, d\mathbf{q}_0\, \rho(\mathbf{P}_0, \mathbf{R}_0) \times W_{|k\rangle}(\mathbf{n}(t))\cdot W_{|i\rangle}(\mathbf{n}_0) \tag{14}$$

(again $\hbar = 1$), where $\rho(\mathbf{P},\mathbf{R})$ is the initial distribution function for the G nuclear DOF, and $W_{|i\rangle}(\mathbf{n})$ (eq 13) is used as the initial distribution function for the F electronic DOF. One can sample initial conditions using these distribution functions, and then for the electronic DOF, typically converts the initial actions $\mathbf{n}_0$ to Cartesian oscillator variables via eq 3 using angles $\{q_k\}$ chosen randomly between 0 and 2π. Trajectories for the full system of nuclear and electronic DOF may then be run using the Cartesian MM Hamiltonian of eq 1 or, as done in this paper and others,[3,5−7] the following symmetrized form may be employed

$$H(\mathbf{P}, \mathbf{R}, \mathbf{p}, \mathbf{x}) = \frac{|\mathbf{P}|^2}{2\mu} + \bar{H}(\mathbf{R}) + \sum_{k<k'}^{F} \left[\frac{1}{2}\left(p_k^2 + x_k^2 - p_{k'}^2 - x_{k'}^2\right)\cdot \frac{H_{k,k}(\mathbf{R}) - H_{k',k'}(\mathbf{R})}{F} + (p_k p_{k'} + x_k x_{k'})\cdot H_{k,k'}(\mathbf{R}) \right] \tag{15}$$

which is obtained by rewriting[13] the diagonal terms relative to the average electronic PES, $\bar{H}(\mathbf{R}) \equiv \frac{1}{F}\sum_k^F H_{kk}(\mathbf{R})$.

Window functions corresponding to all possible final states $\{W_{|k\rangle}(\mathbf{n})\}$ are applied to the time-evolved actions $\mathbf{n}(t)$ calculated using eq 4a at each desired final time t for the ensemble of trajectories. Averaged over the ensemble, this gives a set of raw transition probabilities $\{\tilde{P}_{|k\rangle \leftarrow |i\rangle}(t)\}$ for all possible final states $|k\rangle$ calculated from a given initial state $|i\rangle$. The desired $|f\rangle \leftarrow |i\rangle$ transition probabilities are obtained by renormalizing these results

$$P_{|f\rangle \leftarrow |i\rangle}(t) = \tilde{P}_{|f\rangle \leftarrow |i\rangle}(t) \Big/ \sum_{k=1}^{F} \tilde{P}_{|k\rangle \leftarrow |i\rangle}(t) \tag{16}$$

A compact summary of the SQC quantization procedure is given in Appendix A.

The remaining point to be considered is the parameter γ, which is the only user-defined parameter in the SQC/MM model. In section 2.1, the γ-parameter set the fractional zero-point energy (ZPE) in the MM Hamiltonians of eqs 1 and 2 and in the action-angle/Cartesian transformation equations of eqs 3 and 4 (although γ does not appear in the symmetrized Hamiltonian of eq 15, it still affects the initial conditions through eq 3). Here in section 2.2, it is seen that the same γ-parameter defines the width of the symmetrical windowing functions via eq 11. Thus, through the γ-parameter, the strictness of the imposed symmetrical quantization condition is exactly balanced with the specification of fractional ZPE. This balancing has been found to be an important practical component of the SQC/MM model.

Finally, although we maintain that γ should be viewed as an adjustable parameter, in the SQC/MM treatment of all benchmarks to-date, the same value of γ has been found empirically to be optimal (or at least very nearly so). This selected value of $\gamma = (\sqrt{3} - 1)/2 \approx 0.366$ also has some theoretical justification (as described in ref 3), and it is the value of γ used for every calculation presented in this paper as well.

3. RESULTS

The primary aim of this paper is to apply the SQC/MM approach as just described to the commonly used "site-exciton" (SE) framework for modeling (electronically non-adiabatic) site-to-site energy transfer dynamics in light-harvesting/photosynthetic pigment complexes. These models were used by Ishizaki and Fleming to develop their hierarchical equation of motion (HEOM) approach[8] and also to model the well-known Fenna−Mathews−Olson (FMO) complex.[9] Section 3.1 describes the SE framework in the simplest terms possible as it relates to application of the SQC/MM approach. Section 3.2 presents the SQC/MM treatment of the site-exciton model for 2-states over a wide variety of parameter regimes (8 total). Section 3.3 treats the 7-state FMO problem. Ishizaki and Fleming's HEOM results are presented for comparison for all examples.

3.1. Site-Exciton Models. Within the general site-exciton (SE) framework,[8] each pigment site is modeled as a pair of site-localized electronic states (ground and excited) non-adiabatically coupled to each other and also coupled to a harmonic bath particular to that site (i.e., not coupled to the other sites). Considering just the subspace of single site excitations, the kth electronic state for the entire pigment complex (of F electronic

DOI: 10.1021/acs.jctc.5b01178
J. Chem. Theory Comput. 2016, 12, 983−991

states) then represents a configuration with a single excitation at the kth pigment site (thereby, the different electronic states of the entire pigment complex describe energy transfer from site to site). For $F = 2$ sites/states, the diabatic electronic Hamiltonian's matrix elements corresponding to this model are therefore

$$\{H_{k,k'}(\mathbf{P},\mathbf{Q})\} \equiv \begin{pmatrix} \epsilon_1 & J_{12} \\ J_{12} & \epsilon_2 \end{pmatrix} + \begin{pmatrix} h_{bath}^{(1)}(\mathbf{P},\mathbf{Q}-\mathbf{D}) + h_{bath}^{(2)}(\mathbf{P},\mathbf{Q}) & \varnothing \\ \varnothing & h_{bath}^{(1)}(\mathbf{P},\mathbf{Q}) + h_{bath}^{(2)}(\mathbf{P},\mathbf{Q}-\mathbf{D}) \end{pmatrix} \tag{17}$$

where $\{\epsilon_k\}$ are the site energies, $\{J_{kk'}\}$ the non-adiabatic couplings (assumed to be constants), and

$$h_{\text{bath}}^{(k)}(\mathbf{P},\mathbf{Q}) = \sum_{\xi \in_{\text{modes}}^{\text{site } k}}^{G} \frac{1}{2}P_\xi^2 + \frac{1}{2}\omega_\xi^2 Q_\xi^2 \tag{18}$$

Thus, for $F = 2$ sites, the problem is not very much unlike the well-known "spin-boson" (SB) model treated with the SQC/MM approach in ref 3, though here in this SE framework each cite is coupled to its own bath, and so there are a pair of bath terms appearing in each diagonal element of the 2-site electronic Hamiltonian matrix (only one of which is excited in each matrix element). As with the SB model, quantum coherence effects appear in the SE framework when there is a sufficiently low temperature relative to the non-adiabatic coupling and energetic separation between the states, as effectively set through the thermal distribution given to the initial bath oscillator coordinates $\{Q_\xi\}$ and momenta $\{P_\xi\}$

$$\rho_{\text{bath}}^{(k)}(\mathbf{P},\mathbf{Q}) \propto \prod_{\xi \in_{\text{modes}}^{\text{site } k}}^{G} e^{-\alpha_\xi(\frac{1}{2}P_\xi^2 + \frac{1}{2}\omega_\xi^2 Q_\xi^2)} \tag{19}$$

where $\alpha_\xi = \frac{2}{\omega_\xi}\tanh\left(\frac{\beta\omega_\xi}{2}\right)$.

In Ishizaki and Fleming's model, the bath frequencies $\{\omega_\xi\}$ are assumed to be distributed according to a (standard) Debye spectral density (SD),

$$J(\omega) = 2\lambda\frac{\omega\omega_c}{\omega^2 + \omega_c^2} \tag{20}$$

having characteristic frequency ω_c (the frequency of the SD's peak), and also parametrized by the bath's "reorganization energy" λ.[14] The coupling constants $\mathbf{D} \equiv \{D_\xi\}$ in eq 17 are set by the definition of the reorganization energy

$$\lambda \equiv \sum_\xi \frac{1}{2}\omega_\xi^2 D_\xi^2 \tag{21}$$

and its relationship to $J(\omega)$ implicit in eq 20

$$\lambda = \frac{1}{\pi}\int_0^\infty \frac{J(\omega)}{\omega}\,\mathrm{d}\omega \tag{22}$$

Discretizing eq 22 and equating the terms with eq 21 gives the bath coupling constants as

$$D_\xi = \sqrt{\frac{2}{\pi}J(\omega_\xi)\Delta\omega/\omega_\xi^3} \tag{23}$$

See ref 8 for further details.

For an arbitrary F number of pigment sites, eq 17 generalizes in the obvious way. Note that only one site-specific harmonic bath in each diagonal element is excited (i.e., displaced by $\mathbf{D}$). For example, in the $F = 7$ site/state FMO problem treated below, the electronic Hamiltonian matrix's kth diagonal element is

$$H_{k,k}(\mathbf{Q}) = \epsilon_k + h_{bath}^{(k)}(\mathbf{P},\mathbf{Q}-\mathbf{D}) + \sum_{k'\neq k}^{F=7} h_{bath}^{(k')}(\mathbf{P},\mathbf{Q}) \tag{24}$$

which corresponds to a single excitation on the kth pigment site.

All the calculations presented in this paper employed $G = 200$ bath modes per site (see eq 18). Thus, for 2 sites, the calculations employed $2 \times G = 400$ nuclear DOF plus $F = 2$ electronic DOF, and for the 7-site FMO model, $7 \times G = 1400$ nuclear DOF plus $F = 7$ electronic DOF.

3.2. Results for the 2-Site Model. For the 2-state problem, 8 parameter regimes were considered, as done in ref 8, consisting of 2 values of the bath characteristic frequency ω_c, and for each ω_c, 4 values of the reorganization energy λ, all at a temperature of 300 K and with the non-adiabatic coupling equaling the difference in site energies ($J_{12} = \epsilon_1 - \epsilon_2 = 100$ cm^{-1}).

Figure 1 plots the decay of the initial excitation of electronic state 1 as a function of time for $\omega_c = 53.08$ cm^{-1} (corresponding to a bath time constant of $\tau = 1/\omega_c = 100$ femptoseconds) for the 4 progressively increasing values of λ (= 2, 20, 100, and 500 cm^{-1}) as indicated in the figure. It is seen that the agreement between the SQC/MM calculations and the exact HEOM results is excellent over all 4 regimes. For small λ, the results exhibit significant long-lived oscillations in the transition probabilities, which represent "quantum" coherence between the two electronic states, though it is noted that this electronic coherence is well-replicated here with the purely classical SQC/MM approach (as it was with the spin-boson problems in ref 3). The electronic coherence exhibited in Figure 1 becomes less pronounced as λ is increased because the stronger bath coupling damps the recrossing dynamics, and at $\lambda = 500$ cm^{-1}, the decay is fully monotonic. In each case, the SQC/MM calculations capture the periodicity of the electronic coherence structure as well as the degree to which it is damped with increasing λ. Ironically, it is only in the regime where the electronic coherence is fully damped ($\lambda = 500$) where there is seen to be any real deviation between the SQC/MM and HEOM results.

Figure 2 presents analogous results for the harmonic baths having a much lower characteristic frequency of $\omega_c = 10.61$ cm^{-1} (corresponding to a bath time constant of $\tau = 1/\omega_c = 500$ femptoseconds) and for the same four progressively increasing values of λ (as in Figure 1). Again, it is seen that the SQC/MM approach is in excellent agreement with Ishizaki and Fleming's exact HEOM results. Relative to Figure 1, for some examples, the duration of the electronic coherence structure is extended because the characteristic frequency of the bath is further from resonance with the frequency of the coherence structure (as determined by the site-energies ϵ_1 and ϵ_2 in conjunction with the non-adiabatic coupling J_{12}). Nevertheless, the results are quite similar, exhibiting the same damping of the electronic coherence structure with increasing λ, and once again, it is seen that the only SQC/MM calculation displaying any appreciable

DOI: 10.1021/acs.jctc.5b01178
J. Chem. Theory Comput. 2016, 12, 983−991

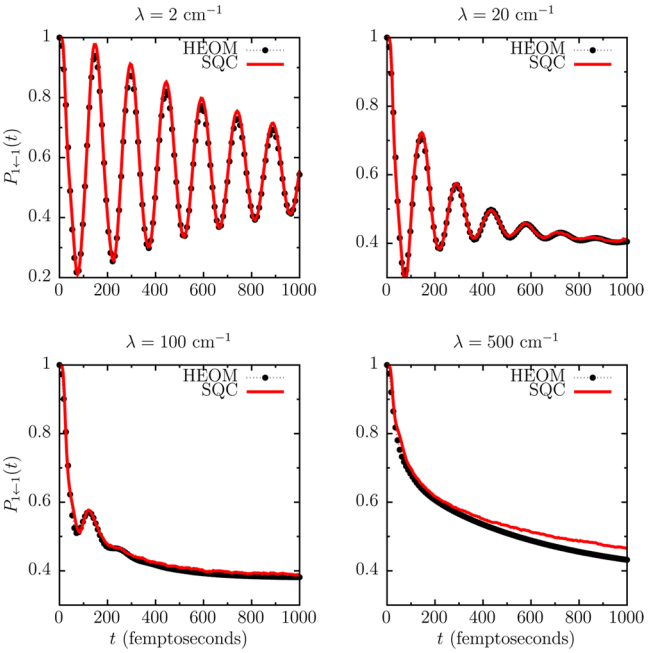

Figure 1. SQC/MM versus HEOM results for 2-state site-exciton model (T = 300 K, $\epsilon_1 - \epsilon_2 = J_{12}$ = 100 cm^{-1}, ω_c = 53.08 cm^{-1}; see Figure 4 of ref 8).

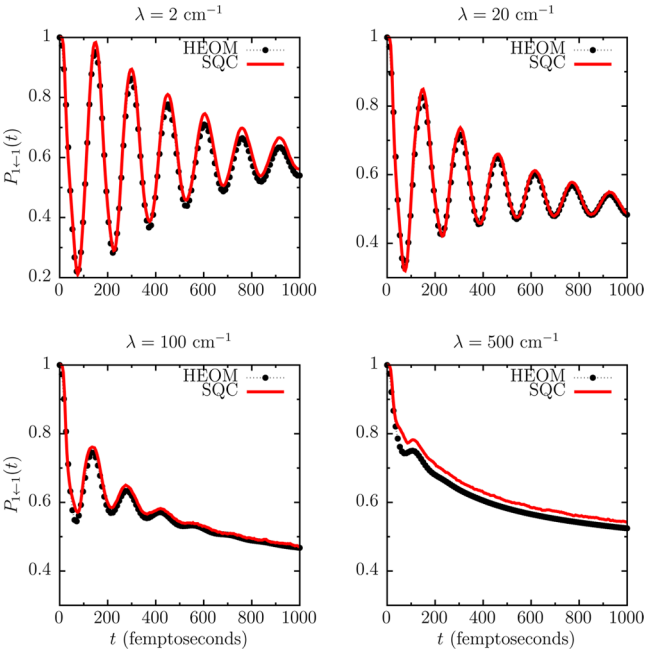

Figure 2. SQC/MM versus HEOM results for 2-state site-exciton model (with parameters the same as Figure 1 except ω_c = 10.61 cm^{-1}; see Figure 6 of ref 8).

deviation from the HEOM results corresponds to the highest value of λ = 500 though, as in Figure 1, the deviation is quite minor.

3.3. Results for the 7-State FMO Pigment Complex.

Although newer model Hamiltonians for the Fenna–Mathews–Olson (FMO) complex have been advocated in the literature (for instance, involving an additional electronic state, more realistic SD functions, etc.), the focus here is on the well-known 7-state model used by Ishizaki and Fleming:[9] with exact HEOM results available for comparison, it serves as a reliable benchmark with which to begin to evaluate the SQC/MM methodology's potential for treating higher numbers of non-adiabatically coupled electronic states. (We note that more recent and more refined HEOM calculations for this model have been carried out by Wilkins and Dattani in ref 15, but for this 7-site model, their results are essentially identical to those of ref 9.)

As described in section 3.1, this 7-state FMO model is analogous to the 2-state problem treated in section 3.2: in particular, each state corresponds to a single excitation located on one of the 7 pigment sites, and the model assumes no coupling between harmonic baths associated with different sites with each bath being described by a Debye SD as given in eq 20. As indicated in section 3.1, the form of the Hamiltonian is the 7-state generalization of eq 17 (i.e., with diagonal elements as shown in eq 24). As given in ref 9, the site energies $\{\epsilon_k\}$ and non-adiabatic couplings $\{J_{k,k'}\}$ are (in cm^{-1})

$$\begin{pmatrix} \epsilon_1 & J_{12} & \cdots & J_{17} \\ J_{21} & \epsilon_2 & & \vdots \\ \vdots & & \ddots & \vdots \\ J_{71} & \cdots & \cdots & \epsilon_7 \end{pmatrix} \equiv \begin{pmatrix} 12410 & -87.7 & 5.5 & -5.9 & 6.7 & -13.7 & -9.9 \\ -87.7 & 12530 & 30.8 & 8.2 & 0.7 & 11.8 & 4.3 \\ 5.5 & 30.8 & 12210 & -53.5 & -2.2 & -9.6 & 6.0 \\ -5.9 & 8.2 & -53.5 & 12320 & -70.7 & -17.0 & -63.3 \\ 6.7 & 0.7 & -2.2 & -70.7 & 12480 & 81.1 & -1.3 \\ -13.7 & 11.8 & -9.6 & -17.0 & 81.1 & 12630 & 39.7 \\ -9.9 & 4.3 & 6.0 & -63.3 & -1.3 & 39.7 & 12440 \end{pmatrix} \quad (25)$$

Because of the larger number of electronic states and non-adiabatic couplings involved in the dynamics (at least potentially), one would generally think that this 7-state problem poses a significantly more challenging benchmark for any simple classical technique to treat properly. It does represent the first reported application by the authors here of the SQC/MM approach to a system having more than 2 electronic states, though it is noted that Tao and co-workers have successfully applied[16] the SQC/MM methodology to models of singlet fission, which involve more than 2 electronic states. However, it turns out that in moving from 2 to 7 electronic states, no modification to the original SQC/MM methodology set forth in ref 3 (and described above in section 2) was required to obtain reasonable results; even the previously used value of γ = 0.366 was found to be optimal (or nearly so).

Two 7-state SQC/MM calculations are presented here in Figures 3 and 4 corresponding to two different initial electronic configurations. Both exhibit significant, but distinctly different, electronic coherence structures between the different states, which is enhanced by the low temperature of 77 K. Other parameters are the same between the two calculations, as indicated in the figure captions, including the bath characteristic frequency of ω_c = 106.14 cm^{-1} (corresponding to $\tau = 1/\omega_c$ = 50 femtoseconds), which represents a shorter time scale than that shown in the 2-state examples.

Figure 3 plots the populations of the 7 electronic states as a function of time after the modeled pigment complex is initialized in electronic state 1. Results are shown for both

DOI: 10.1021/acs.jctc.5b01178
J. Chem. Theory Comput. 2016, 12, 983–991

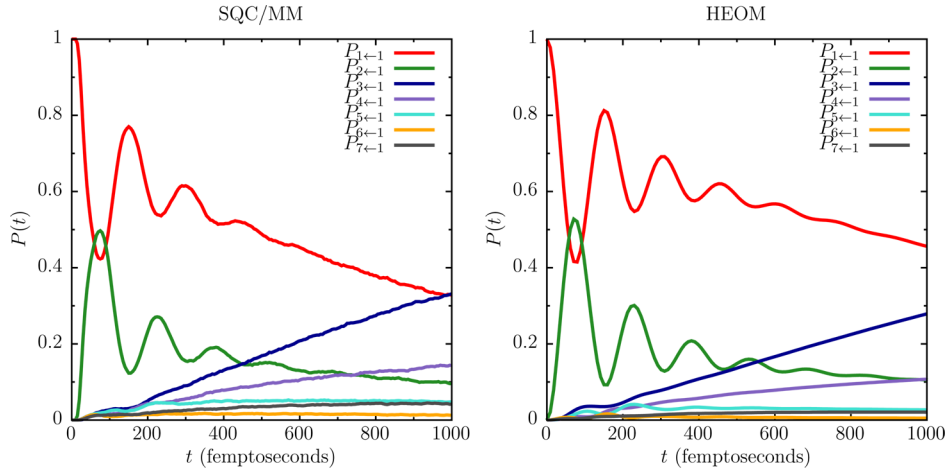

Figure 3. SQC/MM and HEOM results for 7-state FMO model (T = 77 K, λ = 35 cm^{-1}, ω_c = 106.14 cm^{-1}, $\{\epsilon_k\}$ and $\{J_{k,k'}\}$ given in eq 25; see Figure 2a of ref 9).

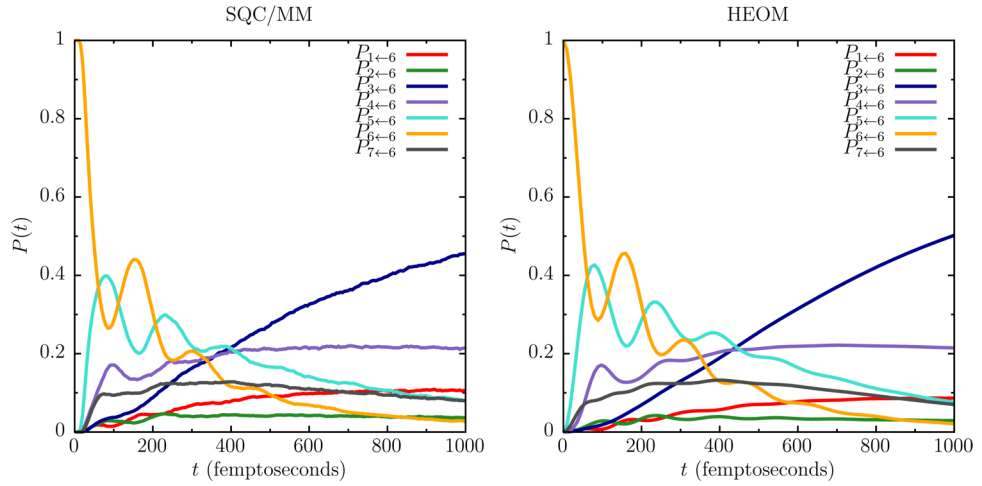

Figure 4. SQC/MM and HEOM results for 7-state FMO model (same as Figure 3 except initialized with site 6 electronically excited; see Figure 2b of ref 9).

the SQC/MM approach and the HEOM technique. The results exhibit significant long-lived coherence structure between electronic states resulting in significant population transfer from state 1 to state 3, and to a lesser degree to state 4, over the course of the 1 picosecond duration plotted in the figure. Overall, the SQC/MM calculation shows remarkable agreement with the exact HEOM results, capturing (probably most importantly) the transfer of the initial electronic excitation from state 1 to states 2−4 (with state 2 serving as a bridge between state 1 and states 3 and 4). There is one significant discrepancy between the two calculations, and that is the long time decay of the population of initial state 1, which is seen to fall a bit too fast in the SQC result relative to the HEOM calculation. Accompanying the greater decay is a slight population bleed into several other states, principally states 3−5 and 7; the effect is small but clearly present (and note that renormalization in the SQC approach forces the sum of the populations to be unity at all times). Nevertheless, the transfer of electronic excitation to states 2−4 is still quite well-described when compared to the exact HEOM result.

Figure 4 shows the analogous SQC/MM calculation when the system is initialized with the electronic excitation localized on pigment 6. In this case, the time-evolution of the electronic coherence structure and the overall multistate dynamics appear far more complex than what is seen in Figure 3: here, 4 of the 7 states exhibit significant coherence structure in the first 200 femptoseconds, and all 7 states have received a not insignificant portion of the initial electronic excitation by the end of the 1 picosecond simulation. Nevertheless, despite the intricacy of the dynamics in this case, the SQC calculation does a remarkable job of replicating the HEOM result, again providing an excellent description of the transfer of electronic excitation to sites 3 and 4 and not exhibiting any obvious substantial deviation from the exact result.

In summary, Figures 3 and 4 provide a good example of the SQC/MM approach applied to a vibronic system having many coupled electronic states that exhibit complex multistate nonadiabatic dynamics, and the results demonstrate (as has now been demonstrated in numerous examples for the case of 2 electronic states) that a very reasonable description of condensed-phase "quantum" coherence effects may be achieved with the SQC/MM technique despite its simplicity and reliance solely on "ordinary" classical mechanics. These are encouraging results, but it should still be borne in mind that for higher numbers of electronic states, in principle, a larger fraction of trajectories will be excluded by the SQC windowing procedure.

DOI: 10.1021/acs.jctc.5b01178
J. Chem. Theory Comput. 2016, 12, 983−991

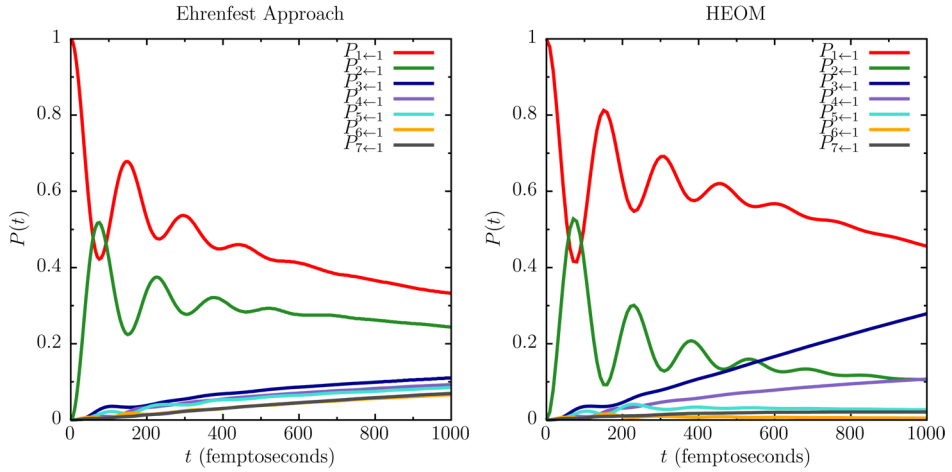

Figure 5. Same as Figure 3 but using the conventional Ehrenfest method.

For these 7-state calculations, only approximately 20% of trajectories are used at a particular time to calculate the electronic state populations (though different trajectories may be used at different times), whereas for the 2-state calculations presented in section 3.2, approximately 60% of trajectories fall within an electronic state window function at any particular time. These are reasonable fractions (particularly as the SQC/MM approach is being extended here to higher numbers of electronic states without any modification), but it is too early to make any generalizations in this regard.

Finally, it is also interesting to see the result one obtains by applying the conventional Ehrenfest approach to the 7-state FMO model. Figure 5 shows the Ehrenfest result when the system is initialized in state 1 (as in Figure 3) side-by-side with the exact HEOM result (from Figure 3). From the comparison, one may conclude that the Ehrenfest approach provides a reasonable description of the electronic coherence structure between states 1 and 2 for short times, but that it fails to capture the transfer of electronic excitation to site 3 over the course of the simulation. More precisely, instead of preferentially routing electronic excitation to site 3, and to a lesser extent to site 4, the Ehrenfest approach appears to direct excitation to sites 3−7 more or less equivalently, thus qualitatively missing an essential feature of the FMO complex's excitation transfer dynamics; one that is well-described in the SQC/MM calculations.

4. SUMMARY AND CONCLUSIONS

The SQC/MM approach presents a simple methodology for the treatment of electronically non-adiabatic processes within the context of classical MD simulation, treating electronic and nuclear degrees of freedom equivalently (via classical mechanics) and thus dynamically consistently. The goal of this work was to apply the SQC/MM approach to the site-exciton framework that is commonly used to model light-harvesting complexes. The results reported here demonstrate for the case of 2 pigments/sites over a wide parameter regime that the SQC/MM approach provides a robust and accurate description of these models. More challenging, of course, is the treatment of higher numbers of pigment sites, and the modeling of multiple site-to-site excitation transfer. Here, it is demonstrated in the context of the 7-state site-exciton model for the FMO complex that the SQC/MM approach is able to handle the case of multisite excitation transfer, and although the results are not absolutely perfect, they do demonstrate the essential features shown in the exact HEOM results, and for the most part with good quantitative accuracy. This is an encouraging finding because up to this point the SQC/MM approach has been benchmarked only against exact results for 2-state models (though others have applied it to higher numbers of states), and no adjustments to the model were needed (even the same value of γ was used) to generate the 7-state results reported here. What is most encouraging about these results, however, is that they suggest the possibility of performing full atomistic trajectory simulations for these site-exciton models, which may incorporate more realistic spectral densities (whether derived experimentally or developed computationally), the use of nonharmonic potential functions, and other modifications to make these multistate site-exciton models more closely resemble true light-harvesting pigment complexes.

Finally, we comment on the number of classical trajectories used to obtain the results presented in the figures above. For the 2-state examples, the results in Figures 1 and 2 were generated from 1×10^5 trajectories; for the 7-state FMO problem, 2.5×10^5 trajectories were used to generate Figures 3 and 4. Although these are not trivial numbers, it should be understood that no attempt was made to minimize the number of trajectories used in these calculations, the primary purpose of this paper being to definitively evaluate the accuracy of the SQC/MM approach for the treatment of the popular site-exciton model. That being said, we have found it generally to be the case (with the SQC/MM approach) that "rough" results may be generated with just a few thousand trajectories. Here, for example, treating the 7-state FMO problem, 2000−5000 trajectories were enough to gauge the general characteristics of the results, which is encouraging when one considers that these 7-state calculations involved a phase-space average over 1400 nuclear DOF. Naturally, one expects that clever importance sampling would improve the statistics significantly, though again, that is beyond the scope of the work done here.

APPENDIX A. STEPS TO APPLY THE MM/SQC APPROACH

To calculate a non-adiabatic transition probability:

I. Evaluate by Monte Carlo (for all energetically feasible final states $|k\rangle$)

DOI: 10.1021/acs.jctc.5b01178
J. Chem. Theory Comput. 2016, 12, 983−991

$$\tilde{P}_{|k\rangle\leftarrow|i\rangle}(t) = \frac{1}{(2\pi)^{G+F}} \int \mathrm{d}\mathbf{P}_0\, \mathrm{d}\mathbf{R}_0\, \mathrm{d}\mathbf{n}_0\, \mathrm{d}\mathbf{q}_0 \rho(\mathbf{P}_0, \mathbf{R}_0)\cdot W_{|k\rangle}(\mathbf{n}_t)\cdot W_{|i\rangle}(\mathbf{n}_0)$$

(i) Chose initial conditions: (a) $\rho(\mathbf{P}_0,\mathbf{R}_0)$ for the G nuclear DOF, (b) $W_{|i\rangle}(\mathbf{n}_0)$ for the F initial actions $\mathbf{n}_0$ ($\mathbf{q}_0$ chosen randomly $[0,2\pi]$) [eq 13]
(ii) Convert $\{n_k(0), q_k(0)\}$ to $\{p_k(0), x_k(0)\}$ [eq 3]
(iii) Propagate to time t using the full MM Hamiltonian [eq 15]
(iv) Calculate $\mathbf{n}_t \equiv \{n_k(t)\}$ from $\{p_k(t),x_k(t)\}$ [eq 4a]
(v) Apply $W_{|k\rangle}(\mathbf{n}_t)$ [eq 13]

II. Renormalize these results for the desired final state $|f\rangle$

$$P_{|f\rangle\leftarrow|i\rangle}(t) = \frac{\tilde{P}_{|f\rangle\leftarrow|i\rangle}(t)}{\sum_k^F \tilde{P}_{|k\rangle\leftarrow|i\rangle}(t)}$$

AUTHOR INFORMATION

Corresponding Authors

*E-mail: StephenJCotton47@gmail.com.
*E-mail: MillerWH@berkeley.edu.

Notes

The authors declare no competing financial interest.

ACKNOWLEDGMENTS

S.J.C. thanks Dr. Jan Roden of the Whaley Research Group at Berkeley for useful and inspiring discussions relating to the site-exciton model of the FMO complex as well as other site-exciton models, and moreover, the types of questions one may begin to ask and answer with trajectory-based methods for treating these systems. S.J.C. also thanks Professor Akihito Ishizaki for providing the HEOM results from refs 8 and 9. This work was supported by the National Science Foundation under Grant No. CHE-1464647 and by the Director, Office of Science, Office of Basic Energy Sciences, Chemical Sciences, Geosciences, and Biosciences Division, U.S. Department of Energy under Contract No. DE-AC02-05CH11231. In addition, this research utilized computation resources provided by the National Energy Research Scientific Computing Center (NERSC), which is supported by the Office of Science of the U.S. Department of Energy under Contract No. DE-AC02-05CH11231.

REFERENCES

(1) Meyer, H.-D.; Miller, W. H. *J. Chem. Phys.* **1979**, *70*, 3214−3223.
(2) Cotton, S. J.; Miller, W. H. *J. Phys. Chem. A* **2013**, *117*, 7190−7194.
(3) Cotton, S. J.; Miller, W. H. *J. Chem. Phys.* **2013**, *139*, 234112.
(4) Marcus, R. A. *J. Chem. Phys.* **1956**, *24*, 966−978.
(5) Cotton, S. J.; Igumenshchev, K.; Miller, W. H. *J. Chem. Phys.* **2014**, *141*, 084104.
(6) Miller, W. H.; Cotton, S. J. *J. Chem. Phys.* **2015**, *142*, 131103.
(7) Cotton, S. J.; Miller, W. H. *J. Phys. Chem. A* **2015**, *119*, 12138−12145.
(8) Ishizaki, A.; Fleming, G. R. *J. Chem. Phys.* **2009**, *130*, 234111.
(9) Ishizaki, A.; Fleming, G. R. *Proc. Natl. Acad. Sci. U. S. A.* **2009**, *106*, 17255−17260.
(10) Stock, G.; Thoss, M. *Phys. Rev. Lett.* **1997**, *78*, 578−581.
(11) Miller, W. H. *J. Chem. Phys.* **1970**, *53*, 3578−3587.
(12) Karplus, M.; Porter, R. N.; Sharma, R. D. *J. Chem. Phys.* **1965**, *43*, 3259−3287.
(13) Note that because $\frac{1}{2}p_k^2 + \frac{1}{2}x_k^2 - \gamma = n_k$ (eq 4a) and because the sum of the actions is conserved and initialized to 1 (or approximately so in the SQC formalism), one may perform the following substitution in the diagonal terms of eq 1

$$\sum_k^F n_k H_{kk}(\mathbf{R}) \rightarrow \bar{H}(\mathbf{R}) + \sum_k^F n_k(H_{kk}(\mathbf{R}) - \bar{H}(\mathbf{R}))$$

to arrive at eq 15. See also ref 3, eqs 5−9.
(14) Note that ω_c was labeled $\gamma = 1/\tau$ in ref 8.
(15) Wilkins, D. M.; Dattani, N. S. *J. Chem. Theory Comput.* **2015**, *11*, 3411−3419.
(16) Tao, G. *J. Phys. Chem. C* **2014**, *118*, 17299−17305.

DOI: 10.1021/acs.jctc.5b01178
J. Chem. Theory Comput. 2016, 12, 983−991